Elastic versus Alloying Effects in Mg-Based Hydride Films

Andrea Baldi*
DIFFER—Dutch Institute for Fundamental Energy Research, De Zaale 20, 5612 AJ Eindhoven, Netherlands

Lennard Mooij, Valerio Palmisano, and Herman Schreuders
Materials for Energy Conversion and Storage, Delft University of Technology, Van der Maasweg 9, 2629 HZ Delft, Netherlands

Gopi Krishnan
Amrita Center for Nanosciences and Molecular Medicine, Amrita Vishwa Vidyapeetham, Kochi, Kerala 682041, India

Bart J. Kooi
University of Groningen, Nijenborgh 4, 9747 AG Groningen, Netherlands

Bernard Dam
Materials for Energy Conversion and Storage, Delft University of Technology, Van der Maasweg 9, 2629 HZ Delft, Netherlands

Ronald Griessen
VU University, De Boelelaan 1081, 1081 HV Amsterdam, Netherlands

(Received 18 July 2018; published 21 December 2018)

Magnesium thin films covered with a layer of Pd absorb hydrogen at much higher pressures than bulk Mg. Such an effect was originally explained as a consequence of elastic clamping on Mg by the capping Pd layer. An alternative interpretation later suggested that the pressure increase could originate from simple alloying between Mg and Pd. Here we resolve this controversy by measuring the hydrogenation and dehydrogenation isotherms of Mg-Pd thin film alloys over a wide range of compositions. Our results disentangle the effects of elastic clamping and alloying and highlight the role of plastic deformations.

DOI: 10.1103/PhysRevLett.121.255503

Several energy storage systems rely on the intercalation of solute atoms into solid host matrices. Tuning the thermodynamics of these solid-state reactions is therefore of paramount importance for designing better energy storage materials [1–3]. For example, while magnesium hydride contains 7.6 mass % of hydrogen, its use in storage applications is limited by slow kinetics of hydrogen absorption and desorption and a high thermodynamic stability [4]. For this reason, several groups have studied ways to modify the stability of MgH_2 either via nanostructuring or by alloying with different elements [5–8]. In 2009, we showed that Mg films covered with a thin layer of Mg-alloy-forming elements, such as Pd and Ni, absorb hydrogen at much higher H_2 gas pressures than bulk Mg [9]. We attributed such destabilization of MgH_2 to the elastic constraints imposed by the capping layer and developed a model to quantitatively interpret our data. In contrast to this explanation, Chung *et al.* later proposed that the observed effect is a mere consequence of alloying at the Mg-Pd interface [10]. Here we solve this controversy by measuring the loading and unloading isotherms of Mg-Pd thin film alloys in a wide range of compositions. In particular, by comparing multiple loading cycles, we demonstrate that alloying with Pd does increase the hydrogenation pressure of Mg, but the effect is unrelated to the clamping mechanism observed for Pd- and Ni-capped films. Strikingly, neither the elastic clamping nor the alloying effects can account for the constant desorption pressure measured for all Mg-Pd alloy compositions. Such behavior points to the importance of plastic deformation and the creation of voids in the microstructure of the films upon cycling with hydrogen.

All thin films are deposited in an ultrahigh vacuum dc or rf magnetron sputtering system (base pressure 10^{-7} Pa) in an argon atmosphere (6N purity, pressure 3 Pa), on substrates kept at room temperature. An $Mg_{1-x}Pd_x$ ($0.02 < x < 0.12$) gradient alloy layer is deposited between two Ti films and the samples are capped with a catalytic Pd layer [Fig. 1(a)]. The Mg, Pd, and Ti targets have purity of 99.95%, 99.98%, and 99.999%, respectively. The Ti layers are intended to isolate the Mg-Pd alloy from the substrate and the palladium on top and minimize any elastic clamping effects [11]. As we will show, while Ti layers are very effective in elastically isolating pure Mg films [11], the negative enthalpy of mixing between Ti and Pd makes them less effective towards

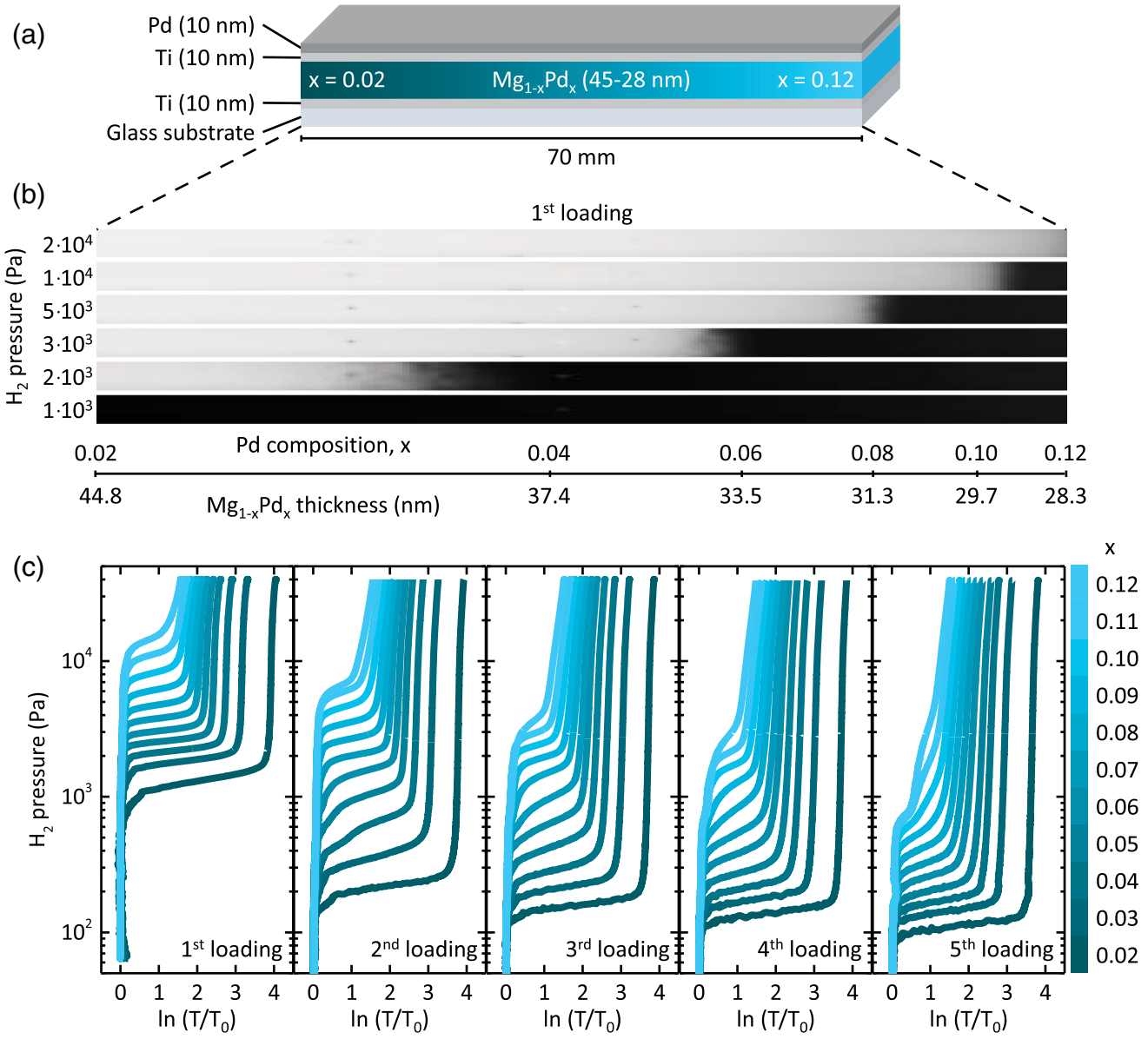

FIG. 1. (a) Sketch of the sample used to measure the hydrogen loading and unloading isotherms of $Mg_{1-x}Pd_x$ alloys ($0.02 < x < 0.12$) in the hydrogenography setup. (b) Top-view optical transmission images collected through the sample at increasing H_2 pressures at 333 K. The images have been stretched horizontally for clarity. (c) Loading PTIs measured at 333 K for selected Mg-Pd alloy compositions in the first five hydrogenation cycles.

Mg-Pd alloys. The Mg-Pd alloy layer is deposited by angled cosputtering of pure Mg and Pd targets on a $70 \times 5 \times 1$ mm quartz wafer substrate. The thickness of the resulting alloy layer varies with composition due to the difference in total deposition rate of Mg and Pd along the 70-mm-long substrate. The thickness of the $Mg_{1-x}Pd_x$ gradient alloy layer is measured with profilometry, while its composition is derived from the calibrated sputtering rates of pure Mg and Pd targets. Such a calibration procedure, validated using Rutherford backscattering spectrometry, provides reliable composition values [12]. The $Mg_{0.9}Pd_{0.1}$ samples for transmission electron microscopy (TEM) analysis are deposited on silicon nitride windows (20 nm thickness, 3×3 mm window array [13]). The Mg-Pd TEM samples have a uniform thickness of 50 nm while the Ti and Pd capping layers are all 3 nm thick, to minimize their influence during imaging. Planar view TEM images are recorded using a JEOL 2010F. Hydrogen absorption and desorption isotherms are measured using hydrogenography, a combinatorial technique that allows recording pressure-optical transmission isotherms (PTIs) for a large number of alloy compositions at once [14]. In a PTI the amount of light transmitted by a thin film is measured as a function of increasing pressure at constant temperature. The

hydrogenography setup consists of a stainless steel cell, with controlled H_2 gas pressure between 10^1 and 10^6 Pa under a flow of 20 sccm. The cell has quartz windows for optical transmission measurements and is placed in a furnace to maintain a constant temperature (here between 333 and 363 K). Depending on the experiment, we use pure hydrogen gas or mixtures containing 0.1% and 4% hydrogen in argon. The light transmitted by the thin films is continuously recorded with a 3-CCD camera (Sony) while varying the H_2 pressure at constant temperature [Fig. 1(b)]. According to the Beer-Lambert law, the logarithm of the transmitted light, normalized by the transmission in the metallic state, is directly proportional to the hydrogen concentration in the film [15].

Figure 1(c) shows the loading PTIs for selected $Mg_{1-x}Pd_x$ compositions, recorded at 333 K during the first five hydrogenation cycles. Higher Pd concentrations lead to significantly higher loading pressures and smaller plateau widths. Interestingly, while for all compositions the loading pressure diminishes upon cycling, the width of the pressure plateaus, expressed in units of $\ln(T/T_0)$, remains roughly constant over multiple hydrogenation cycles [Fig. 2(a)]. From Fig. 2(a) follows that the width of the pressure plateau depends on the Pd concentration in the Mg-Pd alloy. The decrease in plateau width with increasing Pd content is, however, only partially due to the variation in thickness across the Mg-Pd alloy sample. The solid line in Fig. 2(a) shows the plateau width expected under the assumption that Pd does not affect the hydrogen storage capacity of the Mg-Pd alloy and all Mg atoms hydrogenate to form MgH_2. This plateau width is calculated knowing that the hydrogenation of pure Mg to MgH_2 leads to an increase in $\ln(T/T_0)$ of $\sim$0.088 per nm of film thickness [11] (see also the Supplemental Material, Sec. SM1 [16]). From the discrepancy between the solid line and the measured plateau widths for all cycles, it is evident that the presence of Pd in the Mg-Pd alloy prevents the absorption of a significant amount of hydrogen. Assuming that all Mg-Pd alloys form a MgH_2-like rutile structure upon hydrogenation [17,18], in a fully hydrogenated sample each metal atom (Mg or Pd) will be surrounded by 6 hydrogen atoms. The dashed line in Fig. 2(a) plots the predicted plateau width if each Pd atom in the Mg-Pd alloy blocks hydrogen absorption in its 6 nearest neighbors. This corrected plateau width is calculated multiplying the "ideal" width (solid line) by $(1-3x)$. The multiplication factor is correct in the limit of $x \ll 1$, i.e., in the limit of non-neighbouring Pd atoms (see also Supplemental Material, Sec. SM2 [16]). Assuming that each Pd atom prevents the absorption of $\sim$6 hydrogen atoms leads to predicted plateau widths close to the experimentally measured ones and indicates that palladium significantly reduces the hydrogen storage capacity of Mg-Pd alloys. As a consequence, the fact that the plateau widths for Mg-Pd thin films remain roughly constant for the first 5 hydrogen loadings indicates that the overall composition and the chemical short-range order of the Mg-Pd alloys do not significantly change upon cycling [12].

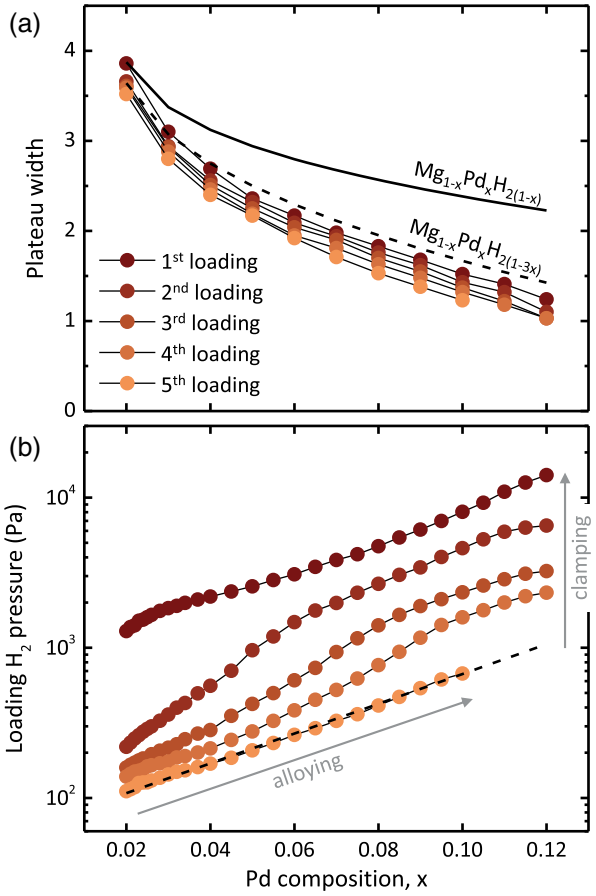

FIG. 2. (a) Width of the nearly horizontal loading plateaus expressed in units of $\ln(T/T_0)$ for the isotherms shown in Fig. 1(c). The solid line corresponds to the expected plateau width, if all the Mg atoms in the Mg-Pd alloy would hydrogenate to form the dihydride MgH_2. The dashed line corresponds to the expected plateau width for a random Mg-Pd alloy in which each Pd atom prevents H occupation of the 6 nearest neighboring sites. (b) Average loading pressures as a function of Pd atomic composition for the first 5 loading cycles. The dashed line is a linear fit to the "ln P versus x" plot during the fifth loading. The fit gives a slope of $\sim$23.

It is then interesting to focus on the evolution of the equilibrium loading plateau pressures over the first five hydrogenation cycles, as shown in Fig. 2(b). There are two distinct effects: (i) in each cycle, higher Pd concentrations lead to higher loading pressures, and (ii) upon cycling the loading pressure for all compositions decreases by more than an order of magnitude. We demonstrate now that the first effect can be quantitatively accounted for by the alloying of Mg and Pd.

Thin films of Mg-Pd alloys have a 002-oriented crystalline structure with x-ray diffraction peaks becoming broader and less intense with higher Pd concentrations and an average lattice parameter roughly corresponding to a Vegard mixture [17] (see Supplemental Material, Sec. SM3

[16]). In first approximation, we neglect electronic contributions to the enthalpy of hydride formation of $Mg_{1-x}Pd_x$ alloys and assume that the effect of mixing with Pd (molar volume $V_{Pd} = 8.8514\ cm^3/mol$) is a mere contraction of the lattice of Mg (molar volume $V_{Mg} = 13.984\ cm^3/mol$). Following Vegard's law, we write the average contraction of the alloy volume as

$$\frac{\partial \ln V}{\partial x} = \frac{V_{Pd} - V_{Mg}}{V_{Mg}} = -0.367. \quad (1)$$

The change in enthalpy of hydride formation as a function of composition is then given by [19]

$$\frac{\partial \Delta H}{\partial x} = \frac{\partial \Delta H}{\partial \ln V}\frac{\partial \ln V}{\partial x} = -B(x)V_H(x)\frac{\partial \ln V}{\partial x} = 0.367B(x)V_H(x), \quad (2)$$

where $B(x)$ and $V_H(x)$ are the composition-dependent bulk modulus and hydrogen partial molar volume for the Mg-Pd alloy, respectively. The bulk modulus of the alloy is expressed as a simple weighted average of the bulk moduli of the constituent elements ($B_{Mg} = 35.4 \times 10^9$ Pa [20], $B_{Pd} = 181 \times 10^9$ Pa [20]),

$$B(x) = (1-x)B_{Mg} + xB_{Pd}, \quad (3)$$

while the partial molar volume of hydrogen in the alloy is taken as the partial molar volume of hydrogen in MgH_2 ($V_{HinMgH_2} = 2.24 \times 10^{-6}\ m^3/mol\,H$ [9]) times the correction factor $(1-3x)$ that accounts for the reduced hydrogen storage capacity due to the presence of Pd,

$$V_H(x) = V_{HinMgH_2}(1-3x). \quad (4)$$

For the range of compositions considered here, $B(x)V_H(x) \approx 80\,kJ/mol\,H$ (see also Supplemental Material, Sec. SM4 [16]). From Eq. (2) we therefore have $\partial\Delta H/\partial x \approx 29\ kJ/mol\,H$. Using the van 't Hoff relationship between the enthalpy of hydride formation ΔH and the hydrogen loading pressure P_{H_2}, we finally obtain

$$\frac{\partial \ln P_{H_2}}{\partial x} = \frac{2}{RT}\frac{\partial \Delta H}{\partial x} \approx \frac{2 \times 29000\ J/mol}{8.314\ J/(K\,mol) \times 333\ K} \approx 21. \quad (5)$$

A linear fit to the composition dependence of the loading pressures for the fifth loading cycle in Fig. 2(b) yields a slope of ~23, in excellent agreement with the predicted theoretical value. Note that a similar slope can also be extrapolated for the first loading cycle. The effect of alloying between Mg and Pd can therefore be quantitatively accounted for by the observed dependence of the loading pressures on the Pd composition x.

By studying the loading isotherms of Mg-Pd alloy thin films, we have so far demonstrated that (i) alloying with Pd leads to higher loading pressures and to a significant reduction of hydrogen uptake in Mg thin films and (ii) cycling with hydrogen does not change the Mg-Pd composition. If the Pd content in Mg does not change upon cycling, however, the decrease in the loading pressures of all Mg-Pd compositions upon multiple hydrogen loadings shown in Fig. 2(b) cannot be due to alloying effects and can only be attributed to (the removal of) elastic clamping effects, as we originally proposed [9,11].

During the first loading, the hydrogen-induced volume expansion of Mg-Pd thin films (~32% for pure MgH_2 [21]) is constrained by the adjacent Ti layers, leading to very high hydrogenation pressures [22]. Such elastic clamping is partially removed during subsequent cycles, due to hydrogen-induced plastic deformations and the creation of structural defects. This scenario is consistent with the measured broadening and decrease in intensity of the x-ray diffraction peaks of Mg-Pd thin film alloys observed upon hydrogen absorption [17]. Interestingly, Pd-poor compositions almost entirely relax these elastic constraints over one hydrogenation cycle, while Pd-rich compositions have slower relaxation rates [Fig. 2(b)]. This trend is consistent with the fact that Pd and Ti atoms form very stable alloys, with an enthalpy of mixing that is significantly more negative than that of Pd with Mg [23]. A larger Pd concentration in the Mg-Pd layer therefore induces a stronger clamping by the adjacent Ti layers [9]. Furthermore, a higher Pd concentration significantly reduces the hydrogen uptake and the consequent plastic deformation of the film, leading to a slower relaxation rate upon cycling.

The lowering of elastic clamping effects upon hydrogen absorption should have dramatic consequences on the dehydrogenation mechanism. This is clearly shown in Fig. 3(a), where we plot equilibrium PTIs for the first three loading cycles and for the fourth unloading cycle of a Mg-Pd alloy thin film. Since hydrogen desorption from thin films is typically slower than hydrogen absorption, the measurements were conducted at a higher temperature of 363 K, to accelerate the reaction kinetics and obtain equilibrium values also for the unloading isotherms [24]. Strikingly, while the loading pressures show a similar dependence on the film's composition as the ones measured at 333 K (Fig. 1), the unloading equilibrium pressures do not exhibit any dependence on the Pd content. The unloading mechanism must therefore be insensitive to the influence of alloying with Pd. In fact, the measured unloading pressure of 3 Pa at 363 K is very close to the one expected for bulk MgH_2 [25].

With the measurement of both loading and unloading isotherms, we can now attempt to draw a complete picture of the mechanism of hydrogen absorption and desorption in our Mg-Pd alloys. Upon hydrogen absorption, Mg-rich

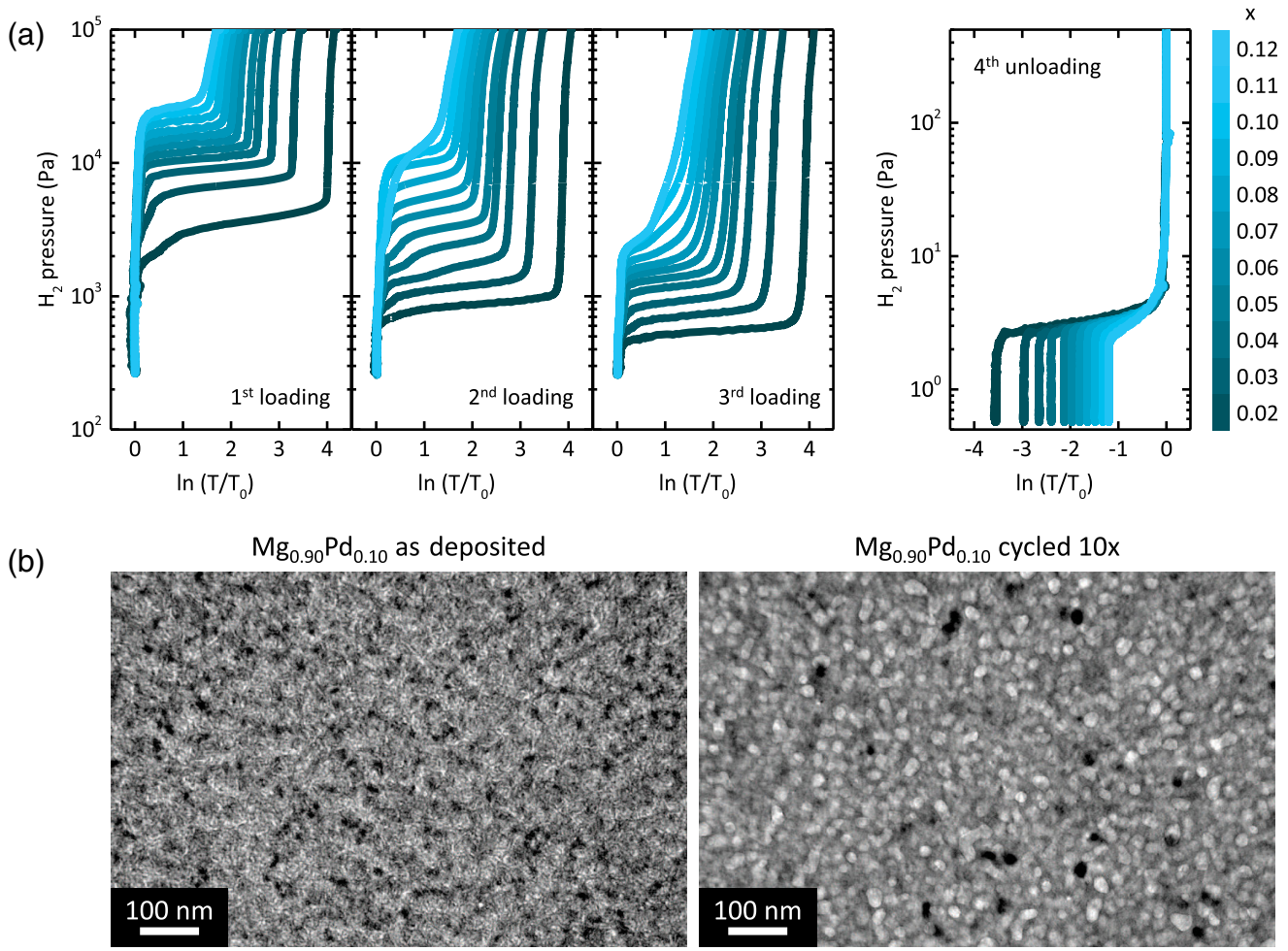

FIG. 3. (a) Pressure-optical transmission isotherms (PTIs) measured at 363 K for the Mg-Pd thin films for the first three loadings and the fourth unloading. Note the different H_2 pressure range for the unloading cycle. (b) Planar view TEM images of a $Mg_{0.9}Pd_{0.1}$ film (left) before and (right) after 10 hydrogenation and dehydrogenation cycles. The sample is supported by a thin Si_3N_4 membrane, and the contribution of the Ti and Pd layers has been minimized using the following structure: Si_3N_4/Ti(2 nm)/$Mg_{0.9}Pd_{0.1}$(50 nm)/Ti(2 nm)/Pd(3 nm).

sites hydrogenate, while Pd-rich sites do not [Fig. 2(a)]. This process decouples the hydrogenated MgH_2-like sites from the Pd-rich ones, which remain in their metallic state. Upon dehydrogenation the lattice volume decreases by ~30% and the MgH_2-like sites are therefore free to desorb hydrogen without any constraint, leading to unloading equilibrium pressures that are independent of the film composition and close to the unloading pressure of pure MgH_2 [Fig. 3(a)] [18,26]. Furthermore, the large volume expansion associated with the uptake of hydrogen must lead to macroscopic structural rearrangements. The associated increase in porosity will weaken the elastic clamping effect on the Mg-Pd alloy from the adjacent Ti layers. In contrast, the alloying influence of Pd is recovered after desorption, as evidenced by the constant slope of the curves in Fig. 2(b). The formation of local structural defects upon hydrogen desorption has already been observed in pure Mg thin films, in which the volume contraction upon dehydrogenation is accompanied by the formation of a porous structure [27–29]. This scenario is confirmed by planar view TEM images of a $Mg_{0.9}Pd_{0.1}$ alloy thin film before and after 10 hydrogenation cycles [Fig. 3(b)]. These TEM images reveal drastic microstructural changes in the metal films upon hydrogen cycling, with coarsening of the grains and the formation of a large number of voids, as confirmed by the appearance of Fresnel fringes while imaging at over and under focus (not shown here). It is evident that the large expansion of Mg-based films upon hydrogenation is not fully relaxed during dehydrogenation and the formation of free surfaces (voids) is more favorable than the plastic deformation needed to fully revert the film back to the initial compact state.

So far, we have shown that the effect of alloying between Mg and Pd on the hydrogenation pressure of Mg-Pd thin films can be fully accounted for by considering the volume contraction due to the addition of smaller Pd atoms to the Mg lattice. By applying the same reasoning to the case of Pd-capped thin films of pure magnesium [9], in which Mg

and Pd form an alloy only at a very thin (less than 2 nm thick) Mg/Pd interface, it is clear that the alloying model of Chung *et al.* [10] cannot explain the observed large increases of hydrogen loading pressure for films as thick as 40 nm. Furthermore, as Mg and Ni have an enthalpy of mixing ($H^{\mathrm{mix}}_{\mathrm{MgNi}} = -5.6$ kJ/mol) that is an order of magnitude smaller than the one of Mg with Pd ($H^{\mathrm{mix}}_{\mathrm{MgPd}} = -43$ kJ/mol) [30,31], the model of Chung *et al.* would predict large differences for the loading pressures of Ni- and Pd-capped Mg films. This prediction is contrary to what we observed experimentally [9]. Interestingly, our elastic clamping model predicts similar increases to the loading pressures of Ni- and Pd-capped Mg thin films, in agreement with the experimental observations. For a more detailed comparison between the clamping [9] and alloying [10] models, see also the Supplemental Materials, Sec. SM5 [16], which includes Ref. [32].

While the clamping model gives a reasonable estimate of the increase in loading pressures of capped thin films, it treats each layer within the elastic approximation and does not take into account any plastic deformation. In light of the composition-independent unloading isotherms shown in Fig. 3(a), however, it is clear that treating the hydrogenation and dehydrogenation of Mg-based films within the elastic approximation is incorrect and that a rigorous treatment should include the energy involved in the creation of plastic deformations. Interestingly, such energy for pure Mg is comparable in magnitude to the elastic energy for a perfectly clamped Pd-Mg bilayer (see Supplemental Material, Sec. SM6 [16], which includes Ref. [33]), at least qualitatively explaining the success of the clamping model in reproducing the observed loading pressures. Finally, a similar asymmetric behavior between hydrogen loading and unloading has already been observed for palladium nanoparticles and interpreted as due to the formation of defects during hydrogen desorption [34].

In conclusion, we have presented a comprehensive study of the effect of alloying on the hydrogen absorption and desorption properties of Pd-doped Mg thin films. Our controlled sample geometry and combinatorial measurement scheme allow us to quantitatively disentangle the effect of alloying from the one due to clamping. Our results demonstrate that, while alloying Mg with Pd does contribute to an increase in loading pressure in Mg-Pd thin films, it cannot explain the 2 orders of magnitude increase in loading pressure observed for Pd-capped Mg films [9]. Our elastic clamping model, however, while quantitatively describing the observed increase in loading pressures, fails to explain why unloading isotherms do not show any composition dependence. Accurate modeling of the hydrogenation process of magnesium-based nanomaterials will have to include the large structural rearrangements and plastic deformations occurring upon hydrogen uptake (see Ref. [35] and the discussion in the Supplemental Material, Sec. SM6 [16]). Furthermore, future efforts to use elastic clamping effects to destabilize hydrogen storage materials will have to take these observations into account. For example, rigid scaffolding systems can only effectively destabilize hydrogen storage systems that undergo small volume expansions upon hydrogenation, therefore remaining within the elastic regime. Alternatively, one could envision a scaffolding system composed of a hydrogen-transparent elastic polymer, capable of accommodating the large volume expansion associated with the hydrogenation process in Mg-based alloys. Finally, our work shows how essential it is that any claim about destabilization of storage materials is substantiated by absorption *and* desorption experiments [36].

This work was supported by the Netherlands Organisation for Scientific Research (Nederlandse Organisatie voor Wetenschappelijk Onderzoek, NWO).

*a.baldi@differ.nl

[1] W. Dreyer, J. Jamnik, C. Guhlke, R. Huth, J. Moškon, and M. Gaberšček, The thermodynamic origin of hysteresis in insertion batteries, Nat. Mater. **9**, 448 (2010).
[2] M. R. Lukatskaya, B. Dunn, and Y. Gogotsi, Multidimensional materials and device architectures for future hybrid energy storage, Nat. Commun. **7**, 12647 (2016).
[3] T. C. Narayan, A. Baldi, A. L. Koh, R. Sinclair, and J. A. Dionne, Reconstructing solute-induced phase transformations within individual nanocrystals, Nat. Mater. **15**, 768 (2016).
[4] L. Schlapbach and A. Zuttel, Hydrogen-storage materials for mobile applications, Nature (London) **414**, 353 (2001).
[5] J. J. Vajo, F. Mertens, C. C. Ahn, R. C. Bowman, and B. Fultz, Altering hydrogen storage properties by hydride destabilization through alloy formation: LiH and MgH_2 destabilized with Si, J. Phys. Chem. B **108**, 13977 (2004).
[6] R. W. P. Wagemans, J. H. Van Lenthe, P. E. De Jongh, A. J. Van Dillen, and K. P. De Jong, Hydrogen storage in magnesium clusters: Quantum chemical study, J. Am. Chem. Soc. **127**, 16675 (2005).
[7] H. Shao, M. Felderhoff, and F. Schuth, Hydrogen storage properties of nanostructured MgH_2/TiH_2 composite prepared by ball milling under high hydrogen pressure, Int. J. Hydrogen Energy **36**, 10828 (2011).
[8] S. A. Shevlin and Z. X. Guo, MgH_2 dehydrogenation thermodynamics: Nanostructuring and transition metal doping, J. Phys. Chem. C **117**, 10883 (2013).
[9] A. Baldi, M. Gonzalez-Silveira, V. Palmisano, B. Dam, and R. Griessen, Destabilization of the Mg-H System through Elastic Constraints, Phys. Rev. Lett. **102**, 226102 (2009).
[10] C.-J. Chung, S.-C. Lee, J. R. Groves, E. N. Brower, R. Sinclair, and B. M. Clemens, Interfacial Alloy Hydride Destabilization in Mg/Pd Thin Films, Phys. Rev. Lett. **108**, 106102 (2012).
[11] A. Baldi, V. Palmisano, M. Gonzalez-Silveira, Y. Pivak, M. Slaman, H. Schreuders, B. Dam, and R. Griessen, Quasifree Mg–H thin films, Appl. Phys. Lett. **95**, 071903 (2009).
[12] R. Gremaud, A. Baldi, M. Gonzalez-Silveira, B. Dam, and R. Griessen, Chemical short-range order and lattice defor-

mations in $Mg_yTi_{1-y}H_x$ thin films probed by hydrogenography, Phys. Rev. B **77**, 144204 (2008).
[13] See TEMwindows.com.
[14] R. Gremaud, C. P. Broedersz, D. M. Borsa, A. Borgschulte, P. Mauron, H. Schreuders, J. H. Rector, B. Dam, and R. Griessen, Hydrogenography: An optical combinatorial method to find new light-weight hydrogen-storage materials, Adv. Mater. **19**, 2813 (2007).
[15] R. Gremaud, M. Slaman, H. Schreuders, B. Dam, and R. Griessen, An optical method to determine the thermodynamics of hydrogen absorption and desorption in metals, Appl. Phys. Lett. **91**, 231916 (2007).
[16] See Supplemental Material at http://link.aps.org/supplemental/10.1103/PhysRevLett.121.255503 for details on the following aspects: SM1: Plateau width as a function of Mg film thickness; SM2: Reduced hydrogen capacity of Mg due to the presence of Pd; SM3: Structural characterization of Mg-Pd alloy thin films with XRD; SM4: Alloying of Mg and Pd: composition dependence of the product B(x) VH(x); SM5: Criticism of the alloying model of Chung et al.; SM6: Elastic energy versus plastic deformation energy.
[17] M. Pasturel, M. Slaman, H. Schreuders, J. Rector, D. Borsa, B. Dam, and R. Griessen, Hydrogen absorption kinetics and optical properties of Pd-doped Mg thin films, J. Appl. Phys. **100**, 023515 (2006).
[18] E. Callini, L. Pasquini, L. Rude, T. Nielsen, T. Jensen, and E. Bonetti, Hydrogen storage and phase transformations in Mg–Pd nanoparticles, J. Appl. Phys. **108**, 073513 (2010).
[19] R. Griessen and R. Feenstra, Volume changes during hydrogen absorption in metals, J. Phys. F **15**, 1013 (1985).
[20] K. A. Gschneidner, Jr., Physical properties and interrelationships of metallic and semimetallic elements, Solid State Phys. **16**, 275 (1964).
[21] F. Manchester, *Phase Diagram of Binary Hydrogen Alloys* (ASM International, Materials Park, OH, 2000).
[22] Note that for a pure Mg film sandwiched between Ti, there is essentially no clamping [9], but for Mg-Pd alloys, Pd can bind to Ti thanks to their negative enthalpy of mixing, and this leads to clamping.
[23] A. R. Miedema, R. Boom,, and F. R. de Boer, On the heat of formation of solid alloys, J. Less-Common Met. **41**, 283 (1975).
[24] L. P. A. Mooij, A. Baldi, C. Boelsma, K. Shen, M. Wagemaker, Y. Pivak, H. Schreuders, R. Griessen, and B. Dam, Interface energy controlled thermodynamics of nanoscale metal hydrides, Adv. Energy Mater. **1**, 754 (2011).
[25] Y. Pivak, H. Schreuders, and B. Dam, Thermodynamic Properties, Hysteresis Behavior and Stress-Strain Analysis of MgH_2 Thin Films, Studied over a Wide Temperature Range, Crystals **2**, 710 (2012).
[26] J. Dufour and J. Huot, Study of Mg_6Pd alloy synthesized by cold rolling, J. Alloys Compd. **446–447**, 147 (2007).
[27] J. A. Dura, S. T. Kelly, P. A. Kienzle, J. H. Her, T. J. Udovic, C. F. Majkrzak, C.-J. Chung, and B. M. Clemens, Porous Mg formation upon dehydrogenation of MgH_2 thin films, J. Appl. Phys. **109**, 093501 (2011).
[28] L. Mooij and B. Dam, Hysteresis and the role of nucleation and growth in the hydrogenation of Mg nanolayers, Phys. Chem. Chem. Phys. **15**, 2782 (2013).
[29] L. J. Bannenberg, H. Schreuders, L. van Eijck, J. R. Heringa, N.-J. Steinke, R. Dalgliesh, B. Dam, F. M. Mulder, and A. A. van Well, Impact of nanostructuring on the phase behavior of insertion materials: The hydrogenation kinetics of a magnesium thin film, J. Phys. Chem. C **120**, 10185 (2016).
[30] F. R. de Boer, R. Boom, W. C. M. Mattens, A. R. Miedema, and A. K. Niessen, *Cohesion in Metals: Transition Metal Alloys* (North-Holland, Amsterdam, 1989).
[31] A. Debski, R. Debski,, and W. Gasior, New features of entall database: Comparison of experimental and model formation enthalpies, Arch. Metall. Mater. **59**, 1337 (2014).
[32] L. Landau and E. Lifshitz, *Theory of Elasticity*, A Course of Theoretical Physics, Vol. 7 (Pergamon Press, Oxford, 1970).
[33] T. B. Flanagan and W. A. Oates, The effect of hysteresis on the phase diagram of Pd-H, J. Less-Common Met. **92**, 131 (1983).
[34] R. Griessen, N. Strohfeldt, and H. Giessen, Thermodynamics of the hybrid interaction of hydrogen with palladium nanoparticles, Nat. Mater. **15**, 311 (2016).
[35] X. Duan, R. Griessen, R. J. Wijngaarden, S. Kamin, and N. Liu, Self-recording and manipulation of fast long-range hydrogen diffusion in quasifree magnesium, Phys. Rev. Mater. **2**, 085802 (2018).
[36] P. Ngene, A. Longo, L. Mooij, W. Bras, and B. Dam, Metal-hydrogen systems with an exceptionally large and tunable thermodynamic destabilization, Nat. Commun. **8**, 1846 (2017).